Seismicity acceleration and clustering before the Mw7.9 Gorkha earthquake, Nepal

Blandine Gardonio, Laurent Bollinger, Marine Laporte, Jérôme Vergne, Helene Lyon-Caen, Lok Bijaya Adhikari

Seismicity acceleration and clustering before the Mw7.9 Gorkha earthquake, Nepal

Blandine Gardonio (blandine.gardonio@univ-lyon1.fr)
Universite de Lyon https://orcid.org/0000-0002-5305-5350
Laurent Bollinger
CEA https://orcid.org/0000-0002-5116-860X
Marine Laporte
Université Lyon 1
Jérôme Vergne
IPGS-EOST
Helene Lyon-Caen
Ecole Normale Superieure, UMR 8538 https://orcid.org/0000-0002-6331-0108
Lok Bijaya Adhikari
Department of Mines and Geology, National Seismological Centre

Article

Keywords: Gorkha earthquake, seismic swarms, pre-seismic phase, template matching

Posted Date: November 30th, 2023

DOI: https://doi.org/10.21203/rs.3.rs-3615145/v1

Additional Declarations: There is **NO** Competing Interest.

Seismicity acceleration and clustering before the M_w7.9 Gorkha earthquake, Nepal

B. Gardonio[1,2*], L. Bollinger[2], M. Laporte[1,2], J. Vergne[3], H. Lyon-Caen[4], L.B. Adhikari[5]

[1*]Univ Lyon 1, ENSL, CNRS, LGL-TPE, F-69622, Villeurbanne, France.
[2]CEA, DAM, DIF, 91297 Arpajon, France.
[3]IPGS-EOST, CNRS/Université de Strasbourg, 67000 Strasbourg, France.
[4]Laboratoire de Géologie, CNRS UMR 8538, Ecole normale supérieure, PSL University, 75005 Paris, France.
[5]Department of Mines and Geology, Nepalese National Earthquake Monitoring and Research Centre, Lainchaur, Kathmandu, Nepal.

*Corresponding author(s). E-mail(s): blandine.gardonio@univ-lyon1.fr;

Abstract

In the last decade, several observations of peculiar seismic and geodetic phases preceding large earthquakes have been documented. Despite being a-posteriori, these observations provide a better understanding of the processes involved in the nucleation of earthquakes. In this study, we investigate the foreshocks and pre-seismic phase of the large M_w7.9 25 April 2015, Gorkha-Nepal earthquake by applying a matched-filter technique on the nucleation zone of the mainshock. We use the seismic signals of 1800 local earthquakes and the continuous signal recorded at the nearest station for the 6 years preceding the mainshock. The pre-seismic phase depicts a long-term increase of seismicity rate and several bursts of micro-earthquakes. The longest swarm occurs one month before the Gorkha earthquake, lasts one week and consists of 38 repetitive earthquakes located at the north western edge of the rupture zone. It is followed by another increase in seismicity rate which starts six days before the mainshock and includes small foreshocks that develop at less than 10 kilometers from the future earthquake hypocenter. These observations suggest that the Gorkha earthquake was preceded by a pre-seismic phase related to a potential initiation of a slow slip with fluids implicated at the northwestern boundary of the rupture zone.

Keywords: Gorkha earthquake, seismic swarms, pre-seismic phase, template matching

1 Introduction

Nepal is located on one of the largest and fastest-slipping continental megathrusts on Earth, the Main Himalayan Thrust (MHT) activated by the continental subduction of the India plate beneath the Tibetan plateau. This tectonic setting results in large devastating earthquakes [3**?**], the largest of these earthquakes rupture the surface, generating plurimetric seismic scarps. Paleoseismological excavations have gradually revealed what happened at the surface termination of these largest earthquakes (e.g.[4]) but the mechanisms at work at depth, and in particular along the deep extension of the fault ruptured, suspected locus of the earthquakes nucleation, remain unknown. The M_w7.9 Gorkha earthquake, on 25 April 2015, is the first Himalayan major event recorded by a permanent and modern network localized above the rupture zone.

This earthquake nucleated near the village of Barpak, in the Gorkha district. Its rupture propagated eastward for about 60 seconds over a 50-km-wide by 140-km-long stretch and the maximum coseismic slip has been estimated to be around 7m, located north of Kathmandu [5–9]. The post-seismic slip dominated by afterslip has been located in the downdip part of the mainshock rupture [10, 11]. The analysis of the numerous aftershocks have shedded lights on the structural complexities of this area [11–20]. The correspondence between the 2015 and the 1833 earthquakes (historical magnitude estimated 7.7) in areas, intensity and magnitude indicate that the same section of the MHT was active at that time. Unlike, the 1833 earthquake that was preceded by two foreshocks felt in Kathmandu 5h and 15 minutes before the mainshock [21], no large foreshocks have been felt by the population before the Gorkha earthquake [22].

There has been several, made a-posteriori, observations of a pre-seismic phase before large earthquakes using seismicity, either on subduction zones [23–28], or in crustal environment [29, 30], although this pre-seismic phase is not always observed and is highly debated [31]. In this study, we address the question of the existence of a pre-seismic phase to the Gorkha earthquake. We use the nearest station of the National Earthquake Monitoring and Research Center (NEMRC) from the Department of Mines and Geology (DMG) network and apply on its records a matched-filter technique on the nucleation zone of the mainshock. We use about 1800 templates, i.e. signals of local earthquakes that happened within 100 kms from the epicenter (Fig. 1). Using this new catalogue, we describe the pre-seismic phase of the continental subduction Gorkha earthquake and propose different models to explain our observations.

2 Main

The NEMRC network is composed of short period and broadband stations sampling at 50Hz, distributed throughout Nepal. The GKN station lies 25 km south of the epicentre of the Gorkha Earthquake, above the MHT. This station is the closest to the mainshock (red triangle in Fig. 1). We use the records from this short period - vertical component- station to search for micro-earthquakes that remained undetected by analysts, in order to complement the time structure of the seismicity (colored circles in Fig. 1b). By first looking at the continuous recording of the GKN station at the time of the mainshock, we find an earthquake of magnitude estimated at 1.3 (see below) that occurred only 28s before the mainshock (Fig. 2).This event has a S-minus-P travel times of 2.86s suggesting that it happened at 23 km from GKN, assuming a Vp/Vs of 1.75 and a Vp around 6 km/s, consistent with the local velocity models. Note that the station signal saturated during the earthquake and an S-time arrival cannot be determined with accuracy. An event preceding the mainshock is also visible on the seismic signal at KKN, further east, with a P-wave arrival time difference between

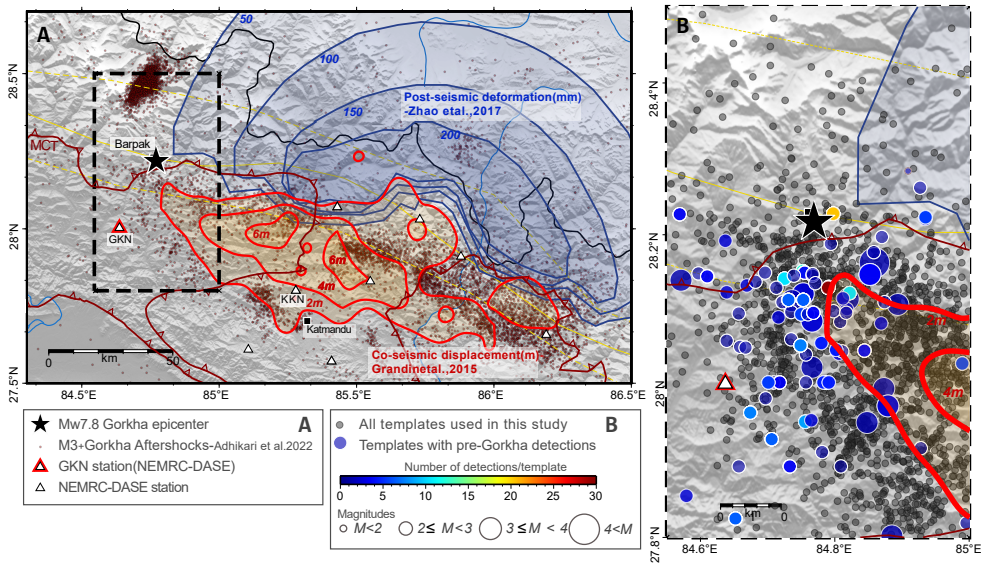

Fig. 1 A: Location of earthquakes and network stations. Red dots show the M≥3 aftershocks earthquakes [19]. The red contours show the seismic slip with 2m intervals starting at 2m [7]. Contours of afterslip are shown in blue [32]. The black star indicates the Gorkha earthquake epicenter. Black triangles indicate the NSC stations and the red triangle indicates the GKN station used in this study. B: In this study, we focus on the initiation part of the rupture zone taking earthquakes that occur both before and after the Gorkha earthquake as templates (grey dots) at the western edge of the rupture. The colored circles shows the templates that detected during this study, colored with their number of detections.

KKN and GKN of 6.8s, identically to the Gorkha earthquake, suggesting that this foreshock happened at close distance from the epicentre (Fig. S1).

We search more systematically for micro-seismic events near the hypocenter of the Gorkha earthquake using the template matching code Obspy (*obspy.signal.cross_correlation*). We use about 1800 templates, occurring between December 2013 and May 2016 (grey circles in Fig. 1B). We use the continuous signal from 2009 to the Gorkha earthquake to compute the correlation between templates and continuous signals in a frequency band of 2-15Hz, taking an 8-second window starting 1 second before the P-wave arrival time. We choose a correlation coefficient threshold of 0.7 and check each detection by eye to avoid false detections. Note that the signals of station GKN were unusable from December 2010 to November 2013.

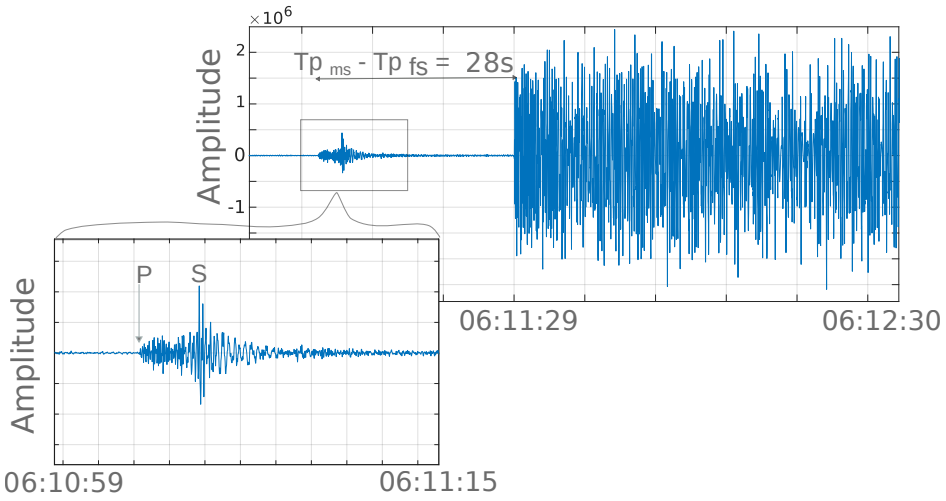

Fig. 2 Record from the GKN station at the time of the Gorkha earthquake. There was an event occurring 28s before the mainshock that has the same difference of P-wave arrival times between GKN and KKN stations than the Gorkha earthquake (see Fig. S1).

The magnitude of template events are local and provided by the NSC. The magnitudes of the newly detected events are calculated during the correlation computation based on the maximum amplitude ratio between the detected and template events by computing a magnitude difference = 4 / 3 * np.log10(amplitude ratio) and adding it to the template magnitude.

Fig. S2a shows an example of detected earthquakes and their stack. Of the 1800 templates used, only 92 are linked with detection of new earthquakes. In this 92, 52 occurred before the mainshock and 40 after it. We obtain a total of 279 detected earthquakes (including the 52 templates that occurred between November 2013 and the Gorkha earthquake).

The distance between a given template and its detections is necessarily very small given the waveforms similarity (we chose a coherency thresholds of 0.7). We therefore consider that the hypocentre of the detections are the same as their corresponding template. The precise hypocentral location of the template could be enhanced through the implementation of event specific relocation technique. We use hypo71 (stars on

Fig.1) using the Nepalese velocity model [33] and putting a weight of 0.5 on S phases, a weight of 1 below 100 km and a linearly decreasing weight down to 0 at 200 km. While we covered the entire western area of the Gorkha earthquake, these newly detected events are mainly located at the western tip of the rupture zone (Fig. 1).

The time series of the cumulative number of earthquakes detected shows different intervals of increased activity (Fig. 3a). Overall, there is an acceleration of the seismicity with time, especially from September 2014 until the mainshock. We compute the cross-correlation between the detected events (Fig. 3b) and show that there are groups occuring in a short time interval that have higher correlation values than the rest (orange and red colors in Fig. 3b).

Period 1 occurs from 02/01/2009 to 19/03/2009, 20 events are detected including a multiplets of seven earthquakes located south to the Gorkha epicenter (light blue dot in Fig. 4a). They are active during a month and also activates later in the analysis (Supplementary Fig.4c and g).

Period 2 gathers 21 earthquakes starting at 23:00 on February 21, 2010 and lasting 48 hours (yellow dot in Fig. 4b). This period contains a group of 16 earthquakes, that are all detected by the same template in 3.5 hours, 14 of them in only an hour (Fig. S3). The cross-correlation values are particularly high and the relative time delays low for the last ten events in the group. Note that the relative magnitudes are small and similar, suggesting that this group may be a seismic swarm. This group is also active during periods 1 and 3 (Fig. 4a and c, yellow dots).

Period 3, from February 23, 2010 to December 12, 2010, contains events with a relatively low inter-correlation, around 0.8-0.85 and a rather stable period with a seismic rate of 0.18 earthquakes per day. The detected earthquakes are clustered south of the Gorkha epicenter, at the western tip of the rupture zone.

Period 4 corresponds to a large swarm of 30 earthquakes occurring in just one hour on the 19/03/2014 between 00h35 and 01h39, mainly detected by three templates

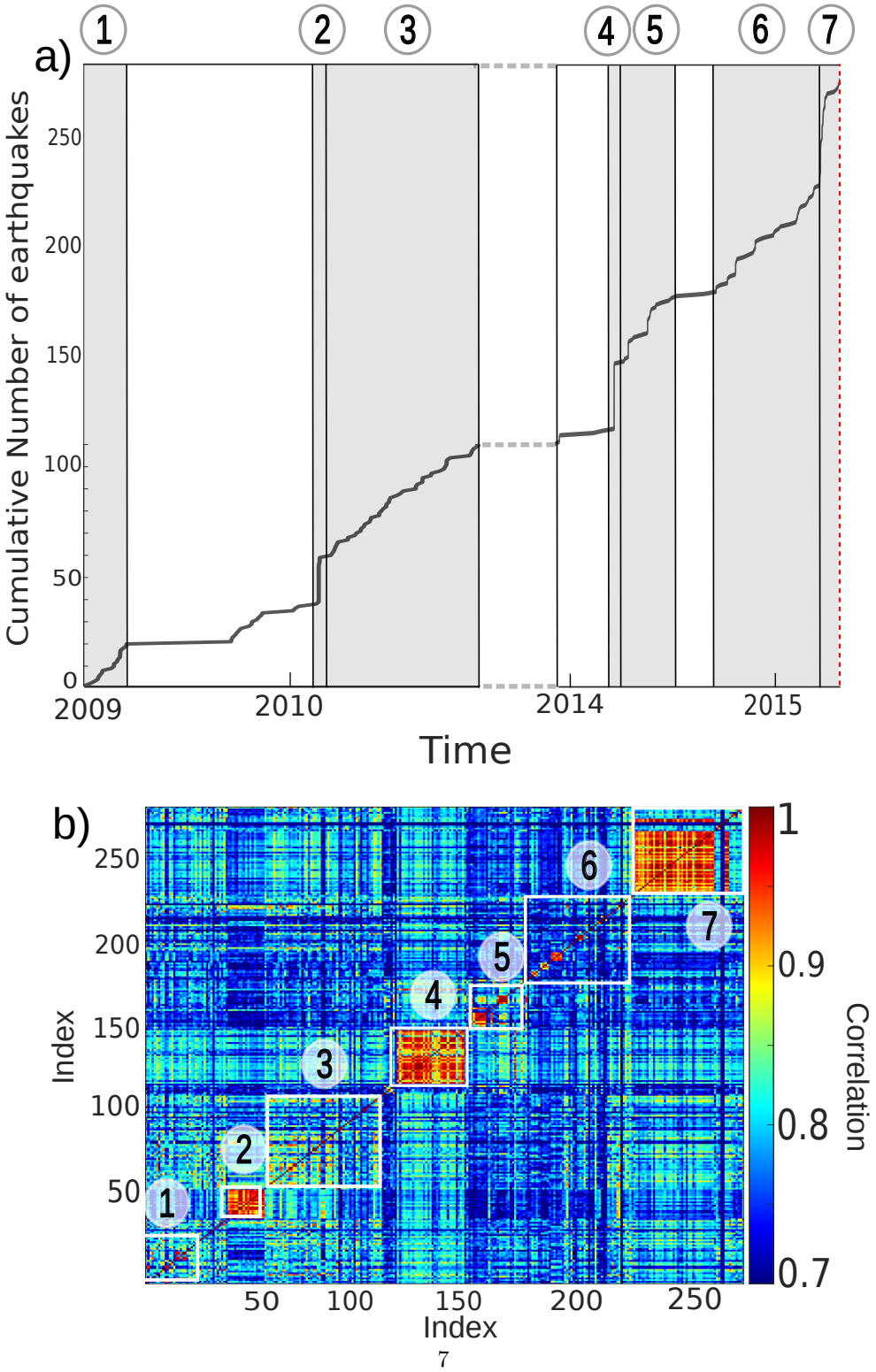

Fig. 3 a) Cumulative number of detected earthquakes with time (gray line) up to the Gorkha earthquake (dashed red line). Note that there was a gap in the seismic data (dashed gray line). Grey periods show significant increases in the seismicity rate. They are numbered at the top and in the correlation matrix (bottom). b) Correlation matrix between all the newly detected earthquakes.

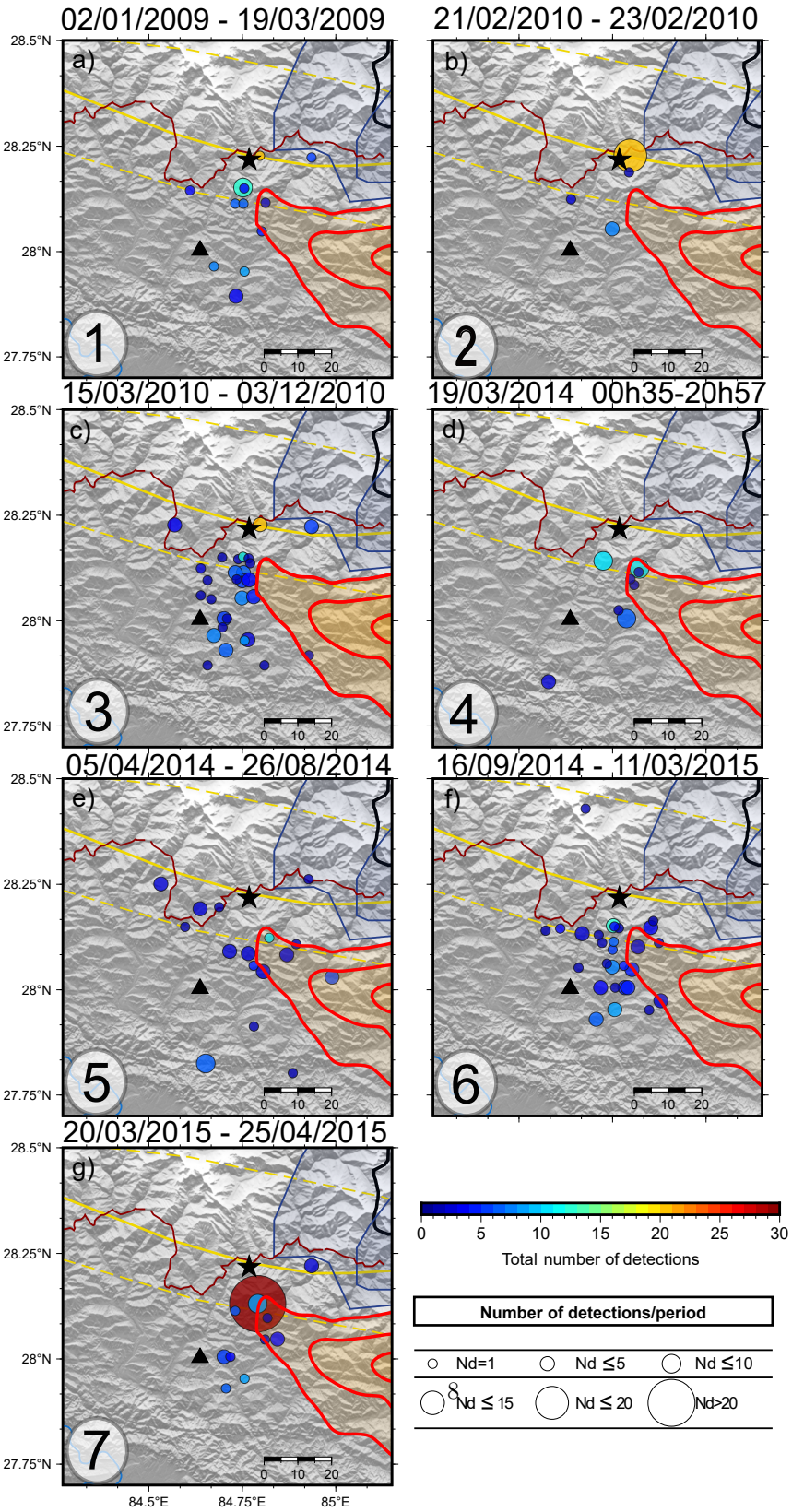

Fig. 4 Snapshots of the seismic activity during the periods of time of Fig. 3. If the template detects during the period, it appears on the snapshot color coded with the total number of detections (over the entire period studied, i.e. 2009-April 2015) and the circle size gives the number of detections during the snapshot only. For example, one template detected a total of 19 earthquakes in periods 1, 2 and 3 (yellow dot in a, b and c), but mainly detected in period 2 (16 earthquakes, b). The black star indicates the epicenter of the Gorkha earthquake, the black triangle locates the GKN station the red contour lines its coseismic slip with a 2m interval starting at 2m.

(Fig. 4d). The inter-correlation values of this group range from 0.8 to 1 with a mean of 0.91 (Fig. S4). Some events in the groups have very large cross-correlation values, with a mean of 0.95, possibly indicating that they are repeating earthquakes. Again, there is no dominant magnitude in this very short sequence. One of the templates is also active in period 5 with an additional detection.

During period 5 from 05/04/2014 to 26/08/2014, two particular sequences occur with two larger earthquakes at the beginning of each sequence (Fig. S5). The first mainshock has a magnitude of 3.7 and occurs on April 13, 2014, triggering 12 earthquakes. The second has a magnitude of 3.4 and occurs on May 17, 2014, triggering a sequence of 20 aftershocks. Both mainshocks were already in the catalogue but not their aftershocks.

During period 6 there is no clustering in time and the inter-correlation values are low. However, there is a clear increase in the seismic rate of 0.26 earthquakes per day and the seismicity is particularly concentrated at the western tip of the Gorkha earthquake.

The last period presents a large swarm with the highest inter-correlation values of the analysis (Fig. 3). This swarm corresponds to 38 earthquakes occurring from the 20/03/2015 to the 02/04/2015, detected by two, very close by, templates (red, magnitude 2.7 and blue, magnitude 3, dots in Fig. 4g) that occur during this sequence. Their magnitudes indicate that their ruptures could have a patch size of about 200-300m. Furthermore, the records of the two templates are very similar when superimposed, and their spectra show the same complexity, suggesting that they are very likely co-located (Fig. 5).The cross-correlation values between the earthquakes of this swarm (ie the two templates and their detections) are high (Fig. S6a). The S-minus-P traveltime is 2.18s (i.e., a distance of 17.5km from GKN) and is very similar for the earthquakes in this swarm. The delay values range from -0.02 to 0.02s (Fig. S6b and c). This swarm

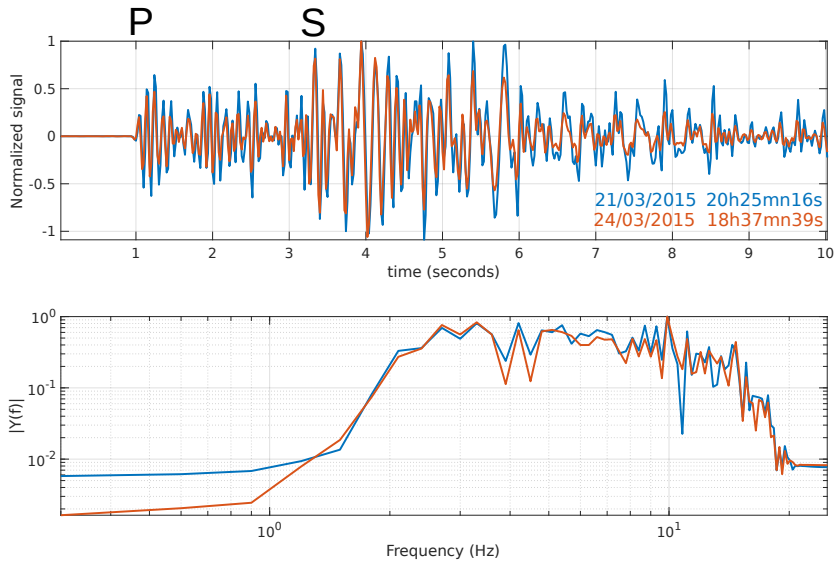

Fig. 5 Top: Superposition of the band-pass filtered (2-20Hz) records of the two largest earthquakes in the sequence of Fig. S6 (magnitude 2.7 and 3, large red circle colocated with a blue one on Fig. 7g) that were already in the NSC catalog, from which 36 new earthquakes were detected. The second waveform has been shifted in time by the time increment that maximizes the cross-correlation of the two signals. Bottom: Comparison of the normalized spectra of the records filtered with a band-pass between 2-20Hz.

of earthquakes is located at the western tip of the coseismic slip inversion, where the rupture initiated [7] (Fig. 4g).

There is a final acceleration during period 7 from the April 19, 2015 to the mainshock with a total of 6 detections, including the small foreshock that occurred only 28s before the mainshock close to the rupture initiation location (Fig. 2).

3 Discussion

Although they can only be defined after the mainshock has occurred, seismic foreshocks are the most relevant observations for understanding the preparation of large earthquakes. We find several swarms of earthquakes that occurred before the Gorkha earthquake and that highlight the perimeter of its western coseismic slip, where the rupture initiated.

Depending on the tectonic setting and structural complexity, three main conceptual models have been developed to explain the pre-seismic phase of large earthquakes: progressive localization of the seismicity, cascade-up, and pre-slip [29, 31, 34–36].

Interestingly, for many large earthquakes that are preceded by a pre-seismic phase, the strain release is progressive, stepwise [23, 24, 37–39]. This is also noteworthy in this study, where we detect several seismic bursts that can be sudden and last only a few hours (periods 2 and 4). During these periods, the seismic events have similar magnitudes, suggesting a swarm-like behavior. Because of their short duration, fluids may be a good candidate for triggering such events [40]. Intermittent fluid release increases the stress on the fault zones and produces local modification of the frictional behavior as seen in rock experiments.

There are multiple indications of fluid presence in the area along the Main Himalayan Thrust (MHT): (a) a seismic low velocity zone (LVZ) coincides with the decollement on that particular section [41], (b) this LVZ is interpreted as a shear zone possibly injected with fluids coming from metamorphic dehydration reactions of sediments thrust over by the hot Himalayan hangingwall, (c) analysis of fluid inclusions from quartz exudates taken within the MCT shear zone, which is a former MHT, demonstrate that both aqueous fluids -mainly brines-, and CO_2-bearing inclusions, originating from metamorphic and meteoric origins, were introduced from mid-crustal to shallower levels [42], (d) the downdip end of the segment of MHT considered corresponds with the position of a low-resistivity anomaly [43], possibly attributed to the presence of saline fluids within fractured rocks.

This body of evidence suggests that aqueous fluids -or supercritical CO_2 -are present at midcrustal depths in the vicinity of the decollement, with the potential to migrate within the fractured rocks of the shear zone as well as along subsidiary faults in its immediate hangingwall [44]. These fluids migrations could be related with

hydrofracturation mechanisms and/or decrease of the friction on the basal decollement, possibly associated to transient decoupling.

We also see a long-term increase of seismic rate between 2010 and 2015 (periods 3 and 6, although the gap in the data makes it difficult to conclude to a long term acceleration). From March 2015, the seismicity increases even more dramatically with the occurrence of 38 repeating earthquakes from 20 March 2015 to 27 March 2015, probably triggered by a slow slip event that lasts a week [23, 24, 29, 37, 45, 46]. After this slow slip event, there is a last acceleration leading up to the mainshock that includes a smaller event close to the hypocenter, in good agreement with the cascade-up model framework [34, 47]. The strain release with a step-like evolution points to a combination of slow slip and fast failure mode foreshocks that locally increase the loading rate of the MHT as seen in rock experiments [48–50] and numerical modeling [51].

The repetitive earthquake activity that preceded the Gorkha mainshock, and the possible transient slow slip associated, could involve various structures at depth. The repeating earthquakes, associated to earthquake templates that happened at mid-crustal depths, occurred necessarily at close distances from the Main Himalayan Thrust, the flat-ramp-flat thrust system which partially ruptured during the mainshock (Fig. 6a-b). In this part of the Himalayas, the geometry of these structures at depth have been inferred from surface exposure of the rocks, [19, 52] and balanced cross section hypothesis, complementing a few geophysical constrains. The position of the upper decollement of the thrust system is associated to the low velocity zone imaged by receiver function analysis [41, 53].

A first plausible scenario involves a transient slow slip and repeating earthquakes on the upper decollement, followed by its partial rupture, from the downdip end of the upper decollement, at the upper edge of the ramp (Fig. 6a-b). The average position of the ramp, at geological timescales, is suspected to develop beneath the front of

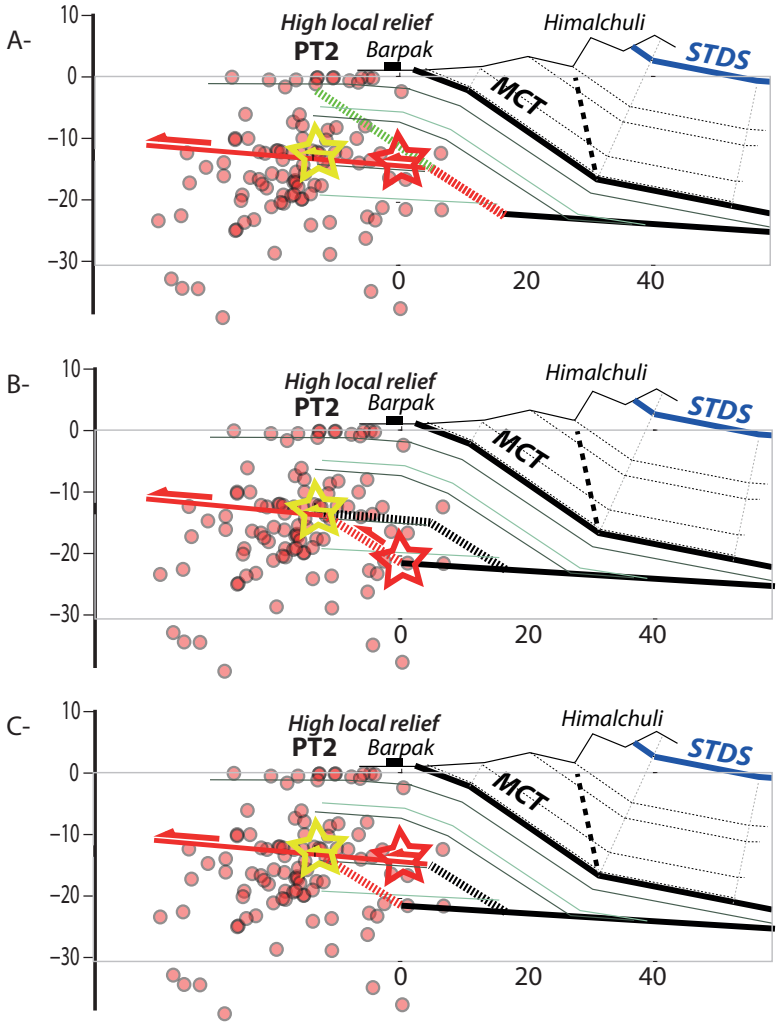

Fig. 6 Interpretative cross sections through the seismicity. The 2015 Gorkha earthquake hypocentre is represented by the red star. The red circles correspond to the location of the earthquakes which were selected as templates. Note that the hypocentral locations of these small earthquakes in the area are associated with very large uncertainties and need to be taken with care: the seismic stations that participate to their location are present to the south of the seismic swarm, leaving large primary azimuthal gaps. The geological structures are constrained by field observations (derived from structural measures of the bedding and schistosity), modified from [19]

the high Himalayas. This is consistent with the thermokinematic evolution recorded by the low temperature thermochronometers (e.g. [52]). However, the present day position of the peak of uplift measured by InSAR and the peak of incision estimated along the rivers since the beginning of the Holocene, suggest that the midcrustal ramp recently migrated southward [54] see Fig. 6c. An alternative to the first scenario, could therefore involve the rupture of this active midcrustal ramp, after a focused repetitive activity at the updip end of the ramp, eventually associated with a slow slip event at the edge of the ramp. A third scenario, involves a seismic activivity in the midcrustal lesser Himalaya duplex. This scenario may involve a focused precursory activity associated with an eventual slow slip at the updip edge of the active ramp, followed by the rupture of the passive roof thrust of the lesser Himalayan duplex (Fig. 6d). These models are difficult to differentiate with the sole seismicity available due to the large uncertainties associated with the earthquake locations. Indeed, the events happen North of Gorkha station and no seismic stations to the North contribute to their location that remain associated to large azimuthal gaps. The seismicity location is therefore associated with significant trade-off between the latitude of the epicenter and the depth of the hypocenter.

4 Conclusion

The application of template matching techniques to the waveforms of the GKN station, the closest station to the epicenter of the Gorkha earthquake, reveals an acceleration of the seismicity rate preceding the earthquake at short distances, within 20 km from its hypocenter. The pre-seismic phase is characterized by the presence of a swarm of earthquakes detected between the 20 March and 27 March 2015, with 38 repeated earthquakes detected by using two very similar templates. This period is followed by the realisation of at least one foreshock that happened 28s before the mainshock.

These observations may be associated with the development of a transient event, mostly aseismic, occurring near the brittle-ductile transition zone, with a few repeating microearthquakes happening at the north western edge of the rupture zone. The event was finally followed by the rupture of the mainshock. Our results show that the Gorkha earthquake belongs to the list of large earthquakes with a pre-seismic phase detected a-posteriori using data mining techniques.

Supplementary information. Figures S1 to S6

Acknowledgments. We acknowledge the cooperation of the Department of Mines and Geology (DMG) - Nepal and CEA/DASE France in the maintenance of the seismological stations used in this study. We are grateful to the team of analysts at NEMRC/DMG, and to Section Chief Bharat Koirala, for their involvement in the processing of the seismicity catalogue. This study was initiated during Lok Bijaya Adhikari's doctoral thesis on the aftershocks of the Gorkha earthquake. **Funding**: BG postdoctoral fellowship was supported by the LRC Yves Rocard (Laboratoire de Recherche Conventionné CEA-ENS- CNRS). **Author contributions**: BG conceived the study. All authors participated to the writing of the manuscript. **Competing interests:** Authors declare no competing interests. **Data and materials availability:** Data available upon request to Blandine Gardonio or Lok Bijaya Adhikari.

References

[1] Sapkota, S. N. *et al.* Primary surface ruptures of the great Himalayan earthquakes in 1934 and 1255. *Nature Geoscience* **6**, 71–76 (2013). URL https://www.nature.com/articles/ngeo1669. Number: 1 Publisher: Nature Publishing Group.

[2] Bollinger, L. *et al.* Estimating the return times of great Himalayan earthquakes in eastern Nepal: Evidence from the Patu and Bardibas strands of the Main Frontal Thrust. *Journal of Geophysical Research: Solid Earth* **119**, 7123–7163 (2014). URL https://onlinelibrary.wiley.com/doi/abs/10.1002/2014JB010970. _eprint: https://onlinelibrary.wiley.com/doi/pdf/10.1002/2014JB010970.

[3] Bilham, R. Himalayan earthquakes: a review of historical seismicity and early 21st century slip potential. *Geological Society, London, Special Publications* **483**, 423–482 (2019). URL https://www.lyellcollection.org/doi/full/10.1144/SP483.16. Publisher: The Geological Society of London.

[4] Riesner, M. *et al.* Surface rupture and landscape response in the middle of the great Mw 8.3 1934 earthquake mesoseismal area: Khutti Khola site. *Scientific Reports* **13**, 4566 (2023). URL https://www.nature.com/articles/s41598-023-30697-7. Number: 1 Publisher: Nature Publishing Group.

[5] Avouac, J.-P., Meng, L., Wei, S., Wang, T. & Ampuero, J.-P. Lower edge of locked Main Himalayan Thrust unzipped by the 2015 Gorkha earthquake. *Nature Geoscience* **8**, 708–711 (2015). URL https://www.nature.com/articles/ngeo2518. Number: 9 Publisher: Nature Publishing Group.

[6] Galetzka, J. *et al.* Slip pulse and resonance of the Kathmandu basin during the 2015 Gorkha earthquake, Nepal. *Science* **349**, 1091–1095 (2015). URL https://www.science.org/doi/10.1126/science.aac6383. Publisher: American Association for the Advancement of Science.

[7] Grandin, R. *et al.* Rupture process of the $M_w = 7.9$ 2015 Gorkha earthquake (Nepal): Insights into Himalayan megathrust segmentation: RUPTURE PROCESS OF THE GORKHA EARTHQUAKE. *Geophysical Research Letters* **42**, 8373–8382 (2015). URL http://doi.wiley.com/10.1002/2015GL066044.

[8] Kobayashi, T., Morishita, Y. & Yarai, H. Detailed crustal deformation and fault rupture of the 2015 Gorkha earthquake, Nepal, revealed from ScanSAR-based interferograms of ALOS-2. *Earth, Planets and Space* **67**, 201 (2015). URL https://doi.org/10.1186/s40623-015-0359-z.

[9] Lindsey, E. O. *et al.* Line-of-sight displacement from ALOS-2 interferometry: Mw 7.8 Gorkha Earthquake and Mw 7.3 aftershock. *Geophysical Research Letters* **42**, 6655–6661 (2015). URL https://onlinelibrary.wiley.com/doi/abs/10.1002/2015GL065385. _eprint: https://onlinelibrary.wiley.com/doi/pdf/10.1002/2015GL065385.

[10] Gualandi, A. *et al.* Pre- and post-seismic deformation related to the 2015, M w 7.8 Gorkha earthquake, Nepal. *Tectonophysics* **714-715**, 90–106 (2017). URL https://linkinghub.elsevier.com/retrieve/pii/S0040195116302207.

[11] Wang, X., Wei, S. & Wu, W. Double-ramp on the Main Himalayan Thrust revealed by broadband waveform modeling of the 2015 Gorkha earthquake sequence. *Earth and Planetary Science Letters* **473**, 83–93 (2017). URL https://www.sciencedirect.com/science/article/pii/S0012821X1730300X.

[12] Adhikari, L. *et al.* The aftershock sequence of the 2015 April 25 Gorkha–Nepal earthquake. *Geophysical Journal International* **203**, 2119–2124 (2015). URL https://doi.org/10.1093/gji/ggv412.

[13] Bai, L. *et al.* Lateral variation of the Main Himalayan Thrust controls the rupture length of the 2015 Gorkha earthquake in Nepal. *Science Advances* **5**, eaav0723 (2019). URL https://www.science.org/doi/full/10.1126/sciadv.aav0723. Publisher: American Association for the Advancement of Science.

[14] Hoste-Colomer, R., Bollinger, L., Lyon-Caen, H., Burtin, A. & Adhikari, L. Lateral structure variations and transient swarm revealed by seismicity along the Main Himalayan Thrust north of Kathmandu. *Tectonophysics* **714-715**, 107–116 (2017). URL https://linkinghub.elsevier.com/retrieve/pii/S0040195116304127.

[15] Mendoza, M. M. *et al.* Duplex in the Main Himalayan Thrust illuminated by aftershocks of the 2015 Mw 7.8 Gorkha earthquake. *Nature Geoscience* **12**, 1018–1022 (2019). URL https://www.nature.com/articles/s41561-019-0474-8. Number: 12 Publisher: Nature Publishing Group.

[16] Yamada, M., Kandel, T., Tamaribuchi, K. & Ghosh, A. 3D Fault Structure Inferred from a Refined Aftershock Catalog for the 2015 Gorkha Earthquake in Nepal. *Bulletin of the Seismological Society of America* **110**, 26–37 (2019). URL https://doi.org/10.1785/0120190075.

[17] Letort, J. *et al.* Teleseismic depth estimation of the 2015 GorkhaNepal aftershocks. *Geophysical Journal International* **207**, 1584–1595 (2016). URL https://doi.org/10.1093/gji/ggw364.

[18] Baillard, C. *et al.* Automatic analysis of the Gorkha earthquake aftershock sequence: evidences of structurally segmented seismicity. *Geophysical Journal International* **209**, 1111–1125 (2017). URL https://doi.org/10.1093/gji/ggx081.

[19] Adhikari, L. B. *et al.* Seismically active structures of the Main Himalayan Thrust revealed before, during and after the 2015 M w 7.9 Gorkha earthquake in Nepal. *Geophysical Journal International* **232**, 451–471 (2022). URL https://academic.oup.com/gji/article/232/1/451/6705419.

[20] Koirala, B. P. *et al.* Tectonic significance of the 2021 Lamjung, Nepal, mid-crustal seismic cluster. *Earth, Planets and Space* **75**, 165 (2023). URL https:

//doi.org/10.1186/s40623-023-01888-3.

[21] Bilham, R. Location and magnitude of the 1833 Nepal earthquake and its relation to the rupture zones of contiguous great Himalayan earthquakes. *Current Science* **69**, 101–128 (1995). URL https://www.jstor.org/stable/24097233. Publisher: Temporary Publisher.

[22] Martin, S. S., Hough, S. E. & Hung, C. Ground Motions from the 2015 Mw 7.8 Gorkha, Nepal, Earthquake Constrained by a Detailed Assessment of Macroseismic Data. *Seismological Research Letters* **86**, 1524–1532 (2015). URL https://doi.org/10.1785/0220150138.

[23] Kato, A. *et al.* Propagation of Slow Slip Leading Up to the 2011 Mw 9.0 Tohoku-Oki Earthquake. *Science* **335**, 705–708 (2012). URL https://www.science.org/doi/abs/10.1126/science.1215141. Publisher: American Association for the Advancement of Science.

[24] Ruiz, S. *et al.* Intense foreshocks and a slow slip event preceded the 2014 Iquique Mw 8.1 earthquake. *Science* **345**, 1165–1169 (2014). URL https://www.science.org/doi/abs/10.1126/science.1256074. Publisher: American Association for the Advancement of Science.

[25] Bouchon, M., Durand, V., Marsan, D., Karabulut, H. & Schmittbuhl, J. The long precursory phase of most large interplate earthquakes. *Nature Geoscience* **6**, 299–302 (2013). URL https://www.nature.com/articles/ngeo1770. Number: 4 Publisher: Nature Publishing Group.

[26] Bouchon, M. *et al.* Potential slab deformation and plunge prior to the Tohoku, Iquique and Maule earthquakes. *Nature Geoscience* **9**, 380–383 (2016). URL https://www.nature.com/articles/ngeo2701. Number: 5 Publisher: Nature

Publishing Group.

[27] Gardonio, B. *et al.* Seismic Activity Preceding the 2011 Mw9.0 Tohoku Earthquake, Japan, Analyzed With Multidimensional Template Matching. *Journal of Geophysical Research: Solid Earth* **124**, 6815–6831 (2019). URL https://onlinelibrary.wiley.com/doi/abs/10.1029/2018JB016751. _eprint: https://onlinelibrary.wiley.com/doi/pdf/10.1029/2018JB016751.

[28] Bouchon, M. *et al.* Observation of rapid long-range seismic bursts in the Japan Trench subduction leading to the nucleation of the Tohoku earthquake. *Earth and Planetary Science Letters* **594**, 117696 (2022). URL https://www.sciencedirect.com/science/article/pii/S0012821X22003326.

[29] Bouchon, M. *et al.* Extended Nucleation of the 1999 Mw 7.6 Izmit Earthquake. *Science* **331**, 877–880 (2011). URL https://www.science.org/doi/full/10.1126/science.1197341. Publisher: American Association for the Advancement of Science.

[30] Gardonio, B., Jolivet, R., Calais, E. & Leclère, H. The April 2017 Mw6.5 Botswana Earthquake: An Intraplate Event Triggered by Deep Fluids. *Geophysical Research Letters* **45**, 8886–8896 (2018). URL https://onlinelibrary.wiley.com/doi/abs/10.1029/2018GL078297. _eprint: https://onlinelibrary.wiley.com/doi/pdf/10.1029/2018GL078297.

[31] Gomberg, J. Unsettled earthquake nucleation. *Nature Geoscience* **11**, 463–464 (2018). URL https://www.nature.com/articles/s41561-018-0149-x. Number: 7 Publisher: Nature Publishing Group.

[32] Zhao, B. *et al.* Dominant Controls of Downdip Afterslip and Viscous Relaxation on the Postseismic Displacements Following the Mw7.9 Gorkha, Nepal, Earthquake. *Journal of Geophysical Research: Solid Earth* **122**, 8376–8401 (2017). URL https://onlinelibrary.wiley.com/doi/abs/10.1002/2017JB014366. _eprint: https://agupubs.onlinelibrary.wiley.com/doi/pdf/10.1002/2017JB014366.

[33] Pandey, M. R. Seismic model of central and eastern Lesser Himalaya of Nepal. *Journal of Nepal Geological Society* **3**, 1–11 (1985). URL https://www.nepjol.info/index.php/JNGS/article/view/32655.

[34] Ellsworth, W. L. & Bulut, F. Nucleation of the 1999 Izmit earthquake by a triggered cascade of foreshocks. *Nature Geoscience* **11**, 531–535 (2018). URL https://www.nature.com/articles/s41561-018-0145-1. Number: 7 Publisher: Nature Publishing Group.

[35] Kato, A. & Ben-Zion, Y. The generation of large earthquakes. *Nature Reviews Earth & Environment* **2**, 26–39 (2020). URL https://www.nature.com/articles/s43017-020-00108-w.

[36] Ben-Zion, Y. & Zaliapin, I. Localization and coalescence of seismicity before large earthquakes. *Geophysical Journal International* **223**, 561–583 (2020). URL https://doi.org/10.1093/gji/ggaa315.

[37] Kato, A. & Nakagawa, S. Multiple slow-slip events during a foreshock sequence of the 2014 Iquique, Chile Mw 8.1 earthquake. *Geophysical Research Letters* **41**, 5420–5427 (2014). URL https://onlinelibrary.wiley.com/doi/abs/10.1002/2014GL061138. _eprint: https://onlinelibrary.wiley.com/doi/pdf/10.1002/2014GL061138.

[38] Socquet, A. *et al.* An 8 month slow slip event triggers progressive nucleation of the 2014 Chile megathrust. *Geophysical Research Letters* **44**, 4046–4053 (2017). URL https://onlinelibrary.wiley.com/doi/abs/10.1002/2017GL073023. _eprint: https://onlinelibrary.wiley.com/doi/pdf/10.1002/2017GL073023.

[39] Nishikawa, T. & Ide, S. Recurring Slow Slip Events and Earthquake Nucleation in the Source Region of the M 7 Ibaraki-Oki Earthquakes Revealed by Earthquake Swarm and Foreshock Activity. *Journal of Geophysical Research: Solid Earth* **123**, 7950–7968 (2018). URL https://onlinelibrary.wiley.com/doi/abs/10.1029/2018JB015642. _eprint: https://onlinelibrary.wiley.com/doi/pdf/10.1029/2018JB015642.

[40] Lengliné, O., Boubacar, M. & Schmittbuhl, J. Seismicity related to the hydraulic stimulation of GRT1, Rittershoffen, France. *Geophysical Journal International* **208**, 1704–1715 (2017). URL https://doi.org/10.1093/gji/ggw490.

[41] Duputel, Z. *et al.* The 2015 Gorkha earthquake: A large event illuminating the Main Himalayan Thrust fault. *Geophysical Research Letters* **43**, 2517–2525 (2016). URL https://onlinelibrary.wiley.com/doi/abs/10.1002/2016GL068083.

[42] Boullier, A.-M., France-Lanord, C., Dubessy, J., Adamy, J. & Champenois, M. Linked fluid and tectonic evolution in the High Himalaya mountains (Nepal). *Contributions to Mineralogy and Petrology* **107**, 358–372 (1991). URL https://doi.org/10.1007/BF00325104.

[43] Lemonnier, C. *et al.* Electrical structure of the Himalaya of central Nepal: High conductivity around the mid-crustal ramp along the MHT. *Geophysical Research Letters* **26**, 3261–3264 (1999). URL https://onlinelibrary.wiley.com/doi/abs/10.1029/1999GL008363. _eprint: https://onlinelibrary.wiley.com/doi/pdf/10.1029/1999GL008363.

[44] Laporte, M. *et al.* Seismicity in far western Nepal reveals flats and ramps along the Main Himalayan Thrust. *Geophysical Journal International* **226**, 1747–1763 (2021). URL https://doi.org/10.1093/gji/ggab159.

[45] Ohnaka, M. Nonuniformity of the constitutive law parameters for shear rupture and quasistatic nucleation to dynamic rupture: a physical model of earthquake generation processes. *Proceedings of the National Academy of Sciences* **93**, 3795–3802 (1996). URL https://pnas.org/doi/full/10.1073/pnas.93.9.3795.

[46] Schurr, B. *et al.* Gradual unlocking of plate boundary controlled initiation of the 2014 Iquique earthquake. *Nature* **512**, 299–302 (2014). URL https://www.nature.com/articles/nature13681.

[47] Yoon, C. E., Yoshimitsu, N., Ellsworth, W. L. & Beroza, G. C. Foreshocks and Mainshock Nucleation of the 1999 Mw 7.1 Hector Mine, California, Earthquake. *Journal of Geophysical Research: Solid Earth* **124**, 1569–1582 (2019). URL https://onlinelibrary.wiley.com/doi/abs/10.1029/2018JB016383. _eprint: https://onlinelibrary.wiley.com/doi/pdf/10.1029/2018JB016383.

[48] Latour, S., Schubnel, A., Nielsen, S., Madariaga, R. & Vinciguerra, S. Characterization of nucleation during laboratory earthquakes. *Geophysical Research Letters* **40**, 5064–5069 (2013). URL https://onlinelibrary.wiley.com/doi/abs/10.1002/grl.50974. _eprint: https://onlinelibrary.wiley.com/doi/pdf/10.1002/grl.50974.

[49] Mclaskey, G. C. & Yamashita, F. Slow and fast ruptures on a laboratory fault controlled by loading characteristics: SLOW AND FAST LABORATORY FAULT RUPTURES. *Journal of Geophysical Research: Solid Earth* **122**, 3719–3738 (2017). URL http://doi.wiley.com/10.1002/2016JB013681.

[50] Xu, S. *et al.* Strain rate effect on fault slip and rupture evolution: Insight from meter-scale rock friction experiments. *Tectonophysics* **733**, 209–231 (2018). URL https://www.sciencedirect.com/science/article/pii/S0040195117305012.

[51] Cattania, C. & Segall, P. Precursory Slow Slip and Foreshocks on Rough Faults. *Journal of Geophysical Research: Solid Earth* **126**, e2020JB020430 (2021). URL https://onlinelibrary.wiley.com/doi/abs/10.1029/2020JB020430. _eprint: https://onlinelibrary.wiley.com/doi/pdf/10.1029/2020JB020430.

[52] Ghoshal, S., McQuarrie, N., Huntington, K. W., Robinson, D. M. & Ehlers, T. A. Testing erosional and kinematic drivers of exhumation in the central Himalaya. *Earth and Planetary Science Letters* **609**, 118087 (2023). URL https://www.sciencedirect.com/science/article/pii/S0012821X23001000.

[53] Nábělek, J. *et al.* Underplating in the Himalaya-Tibet Collision Zone Revealed by the Hi-CLIMB Experiment. *Science* **325**, 1371–1374 (2009). URL https://www.science.org/doi/abs/10.1126/science.1167719. Publisher: American Association for the Advancement of Science.

[54] Grandin, R. *et al.* Long-term growth of the Himalaya inferred from interseismic InSAR measurement. *Geology* **40**, 1059–1062 (2012). URL https://doi.org/10.1130/G33154.1.

Supplementary Files

This is a list of supplementary files associated with this preprint. Click to download.

- preGorkhaSuppMat.pdf